



Deletion of Arginase 2 Ameliorates Retinal Neurodegeneration in a Mouse Model of Multiple Sclerosis

Chithra D. Palani^{1,2} · Abdelrahman Y. Fouda^{2,3} · Fang Liu^{1,2} · Zhimin Xu^{2,3} · Eslam Mohamed^{4,5} · Shaileendra Giri⁶ · Sylvia B. Smith^{2,7} · Ruth B. Caldwell^{2,3,7,8} · S. Priya Narayanan^{1,2,3,8} 

Received: 23 April 2019 / Accepted: 25 June 2019 / Published online: 6 July 2019
© Springer Science+Business Media, LLC, part of Springer Nature 2019

Abstract

Optic neuritis is a major clinical feature of multiple sclerosis (MS) and can lead to temporary or permanent vision loss. Previous studies from our laboratory have demonstrated the critical involvement of arginase 2 (A2) in retinal neurodegeneration in models of ischemic retinopathy. The current study was undertaken to investigate the role of A2 in MS-mediated retinal neuronal damage and degeneration. Experimental autoimmune encephalomyelitis (EAE) was induced in wild-type (WT) and A2 knockout (A2^{-/-}) mice. EAE-induced motor deficits, loss of retinal ganglion cells, retinal thinning, inflammatory signaling, and glial activation were studied in EAE-treated WT and A2^{-/-} mice and their respective controls. Increased expression of A2 was observed in WT retinas in response to EAE induction. EAE-induced motor deficits were markedly reduced in A2^{-/-} mice compared with WT controls. Retinal flat mount studies demonstrated a significant reduction in the number of RGCs in WT EAE retinas in comparison with normal control mice. A significant improvement in neuronal survival was evident in retinas of EAE-induced A2^{-/-} mice compared with WT. RNA levels of the proinflammatory molecules CCL2, COX2, IL-1 α , and IL-12 α were significantly reduced in the A2^{-/-} EAE retinas compared with WT EAE. EAE-induced activation of glia (microglia and Müller cells) was markedly reduced in A2^{-/-} retinas compared with WT. Western blot analyses showed increased levels of phospho-ERK1/2 and reduced levels of phospho-BAD in the WT EAE retina, while these changes were prevented in A2^{-/-} mice. In conclusion, our studies establish EAE as an excellent model to study MS-mediated retinal neuronal damage and suggest the potential value of targeting A2 as a therapy to prevent MS-mediated retinal neuronal injury.

Keywords Arginase 2 · Retina · Optic neuritis · Neurodegeneration · EAE · Retinal ganglion cells

Abbreviations

A2 Arginase 2
A2^{-/-} A2 knockout
GCC Ganglion cell complex

EAE Experimental autoimmune encephalomyelitis
GCL Ganglion cell layer
IPL Inner plexiform layer
INL Inner nuclear layer

Chithra D. Palani, Abdelrahman Y. Fouda and Fang Liu contributed equally to this work.

Electronic supplementary material The online version of this article (<https://doi.org/10.1007/s12035-019-01691-w>) contains supplementary material, which is available to authorized users.

✉ S. Priya Narayanan
pnarayanan@augusta.edu

¹ Clinical and Experimental Therapeutics, College of Pharmacy, University of Georgia, Augusta, GA 30912, USA

² Culver Vision Discovery Institute, Augusta University, Augusta, GA 30912, USA

³ Vascular Biology Center, Augusta University, Augusta, GA 30912, USA

⁴ Georgia Cancer Center, Augusta University, Augusta, GA 30912, USA

⁵ Present address: Department of Immunology, Moffitt Cancer Center, Tampa, FL 33612, USA

⁶ Department of Neurology, Henry Ford Health System, Detroit, MI 48202, USA

⁷ Department of Cellular Biology and Anatomy, Augusta University, Augusta, GA 30912, USA

⁸ Charlie Norwood VA Medical Center, Augusta, GA 30904, USA

MS	Multiple sclerosis
OPL	Outer plexiform layer
ONL	Outer nuclear layer
OCT	Optical coherence tomography
PFA	Paraformaldehyde
RGCs	Retinal ganglion cells
RNFL	Retinal nerve fiber layer
WT	Wild type

Introduction

Multiple sclerosis (MS) is a chronic inflammatory disease of the central nervous system characterized by demyelination, inflammatory responses, and neurodegeneration. MS patients suffer from various disabilities such as vision problems, memory loss, cognitive deficit, and movement disorders. Visual dysfunction is one of the most common clinical manifestations of MS. There is a growing interest to include sensitive measures of visual function and retinal thickness in MS clinical trials such as optical coherence tomography, magnetic resonance imaging, and electrophysiological measures [1, 2].

Visual dysfunction in MS results from optic neuritis and MS-induced pathology can lead to temporary or permanent vision loss. Optic neuritis is characterized by thinning of the nerve fiber layer, degeneration of retinal ganglion cells (RGCs), and loss of inner retinal function secondary to optic nerve degeneration [3–6]. Current medications available for treating MS are only partially effective as they specifically target the inflammatory phase, but not the neurodegenerative phase, and therefore have limited effects on long-term disability [7, 8]. During the past decade, many advancements have occurred in the field of MS treatment. There are several disease-modifying therapies (DMTs) approved for the treatment of MS in the USA. However, none of these agents are proven to be neuroprotective, so the need for better treatment strategies for MS remains. Major treatment options include interferon beta (IFN β) and glatiramer acetate (GA). Fingolimod, which is approved in 2010 in USA, is the first oral DMT. Since then, a number of other oral medications have been validated or are in clinical trials [9, 10]. Currently, three monoclonal antibodies are approved for MS therapy, and some other agents are in the final phase of development. Although significant progress in MS treatment has occurred, it is not clear whether the current medications will address the future needs of MS-associated disabilities. There is a great need for identifying new agents that target both inflammatory and neurodegenerative phases of the disease.

Experimental autoimmune encephalomyelitis (EAE) is a widely used rodent model to study MS-associated pathophysiology including optic neuritis [11–15]. Both MS and EAE are characterized by inflammation and neurodegeneration. Previous studies have shown that EAE mice develop retinal

inflammation, RGC loss, Müller cell activation, and infiltration of macrophages [16–19]. However, the molecular mechanisms by which EAE mediates retinal inflammation and neuronal damage are still to be elucidated.

Arginase is a metalloenzyme, which converts L-arginine to urea and ornithine. Excessive arginase activity has been reported in pathologies associated with cardiovascular diseases, diabetes, hypertension, and aging [20]. Arginase has two isoforms, arginase 1 (A1) which is cytosolic and primarily expressed in the liver where it mediates ammonia detoxification and arginase 2 (A2) which is mitochondrial and primarily expressed in the kidney. Both isoforms are also expressed in the brain and retina and have been implicated in the pathophysiology of several neurodegenerative conditions [20]. Our laboratory has previously demonstrated the involvement of arginase in retinal neuronal damage and dysfunction. We have shown that deletion of A2 significantly reduced neurodegeneration and improved retinal function in a mouse model of oxygen-induced retinopathy (OIR) [21]. A2 deletion also significantly improved RGC survival in a model of retinal ischemia-reperfusion (IR) injury [22]. Our recent study using a model of traumatic optic neuropathy (TON) further demonstrated the beneficial effect of A2 deletion on RGCs survival [23].

In the current study, we examined the protective effect of A2 deletion on EAE-induced neurodegeneration in the retina. A combination of clinical scoring, molecular analyses, and imaging techniques were employed to investigate the impact of A2 deletion in the EAE retina during the disease.

Materials and Methods

Animals and Induction of EAE

All animal procedures complied with the ARVO statement for the use of Animals in Ophthalmic and Vision Research. Female (12 weeks old) wild-type (WT) C57BL/6J and arginase 2 knockout (A2^{-/-}) mice on C57BL/6J background were maintained in our animal facility and used in this study. Chronic EAE was induced using Hooke EAE induction kit (Hooke Laboratories, Lawrence, MA, cat. no. EK-2110), and according to the previously published method with minor modifications [24]. Briefly, mice were immunized on day 0 by subcutaneous injections in the flank region with a total of 200 μ l of emulsion containing myelin oligodendrocyte glycoprotein (MOG_{35–55}) peptide (200 μ g/mouse) along with complete Freund's adjuvant (CFA, killed *Mycobacterium tuberculosis* H37Ra (final concentration 400 μ g/ μ l)). Additionally, each mouse received 100 ng of pertussis toxin (PTX) by i.p. injection in 50 μ l of PBS on day 0 (1–2 h after MOG_{35–55}/CFA injection) and day 1 post-immunization (total dose given of PTX is 200 ng). PTX was freshly diluted each

day in cold PBS. Control group was immunized with CFA without antigen (MOG peptide) while two doses of PTX were given on day 0 and day 1. This protocol resulted in four groups; group 1 (WT control): WT mice immunized with CFA with two injections of PTX, group 2 (WT EAE): WT mice immunized with MOG in CFA with two injections of PTX, group 3 (A2^{-/-} control): A2^{-/-} mice immunized with CFA with two injections of PTX, and group 4 (A2^{-/-} EAE): A2^{-/-} mice immunized with MOG in CFA with two injections of PTX.

Clinical disease was monitored daily in a blinded fashion by measuring paralysis according to the following conventional grading system: 0, no disease; 1, complete loss of tail tonicity; 2, partial hind limb paralysis (uneven gait of hind limb); 3, complete hind limb paralysis; 4, complete hind and forelimb paralysis; and 5, moribund or dead [24]. Animals displaying paralysis on all four limbs and/or weight loss more than 15% were sacrificed. Soft food was provided in the cage for paralyzed mice. At various time points after EAE (or control) induction, mice were euthanized by overdose with ketamine/xylazine cocktail and eyeballs or retinas were harvested and prepared for analysis. The experimental design and analysis endpoints are shown in Fig. 1a.

Quantitative RT-PCR

Total retinal RNA extract was prepared and reverse-transcribed as previously described [22]. Quantitative PCR was conducted using ABI StepOnePlus Thermocycler (Applied Biosystems, Foster City, CA) using master mix

(Power SYBR Green, Invitrogen, Carlsbad, CA). Mouse primer sequences are shown in Table 1. Data were normalized to hypoxanthine phosphoribosyltransferase (HPRT), and the fold change between levels of different transcripts was calculated by the $\Delta\Delta C_T$ method.

Spectral Domain Optical Coherence Tomography Analysis

Thickness of retina and retinal layers was assessed using optical coherence tomography (OCT). Mice were anesthetized using ketamine/xylazine (73 mg/kg ketamine hydrochloride and 7.3 mg/kg xylazine hydrochloride, i.p.; Sigma-Aldrich Corp., St. Louis, MO). Pupils were dilated with 1% tropicamide (Bausch & Lomb, Tampa, FL) followed by application of GenTeal Lubricant Eye Gel (Alcon, Fort Worth, TX). B-scan images were taken using the Bioptigen Spectral Domain Ophthalmic Imaging System (SDOIS) (Bioptigen Envisu R2200, NC) as we previously described [25]. Average values of retinal layers' thickness were generated using InVivoVue software (Bioptigen Inc.).

Western Blotting

Retinas were collected and homogenized in RIPA buffer (Millipore, Burlington, MA) containing protease and phosphatase inhibitors (Complete Mini and phosSTOP Roche Applied Science, Indianapolis, IN). Retinal protein lysates were run on SDS-PAGE and transferred to nitrocellulose membranes (Millipore). Membranes were blocked in 5% milk

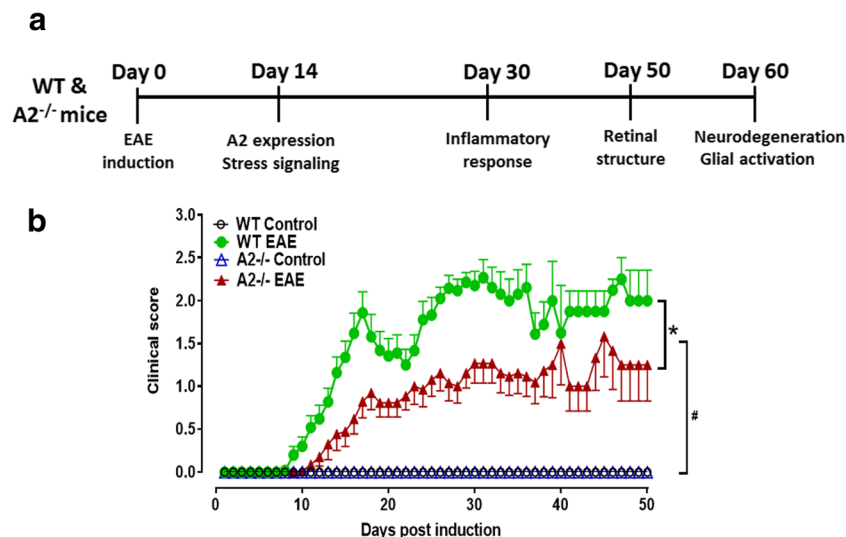


Fig. 1 EAE induction and evaluation of clinical scores. **a** Schematic representation of the time points of EAE induction and experiments performed. **b** Animals were evaluated every day, and the clinical scores were recorded according to a 0–5 scale (see “Materials and Methods” section for details). WT EAE mice showed progressively increasing clinical score starting at day 9. A2^{-/-} EAE mice showed significantly lower clinical score as compared with WT EAE mice. Both control

groups showed no signs of motor deficits. * $p < 0.05$, A2^{-/-} EAE vs WT EAE for days 11–21, 24–37, 41–43, and 47. # $p < 0.05$, WT and A2^{-/-} EAE groups vs respective control groups starting at days 11 and 14, respectively, and till the end of the experiment. $N = 17$ –26 per group. Four animals in WT EAE and two in A2^{-/-} EAE group died or were sacrificed due to weight loss. Data are presented as mean \pm SEM

Table 1 Primer sequences used in the study

Gene name	Assay ID	Company
IL12 α	Mm00434165_m1	Life Technologies Corp., Grand Island, NY
IL1 α	Mm00439620_m1	Life Technologies Corp., Grand Island, NY
COX2	Mm03294838_g1	Life Technologies Corp., Grand Island, NY
CCL2	Mm00441242_m1	Life Technologies Corp., Grand Island, NY
IL-10	Mm01288386_m1	Life Technologies Corp., Grand Island, NY
Arginase 1	Mm00475988_m1	Life Technologies Corp., Grand Island, NY
HPRT	Mm00446968_m1	Life Technologies Corp., Grand Island, NY
IL18	Forward primer: TCAAAGTGCCAGTGAACCCC Reverse primer: GGTCACAGCCAGTCCTTAC	SA Biosciences, Germantown, MD
TNF α	Forward primer: GGTCACAAAGGGATGAGAA Reverse primer: TGAGGGTCTGGGCCATAGAA	SA Biosciences, Germantown, MD
HPRT	Forward primer: GAAAGACTTGCTCGAGATGTCATG Reverse primer: CACACAGAGGGCCACAATGT	SA Biosciences, Germantown, MD

(Bio-Rad, Hercules, CA) in Tris-buffered saline with 0.05% Tween-20 (TBS-T) and incubated with primary antibodies (Table 2) overnight at 4 °C. The membranes were further incubated with horseradish peroxidase-conjugated secondary antibodies (GE Healthcare Bio-Science Corp., Piscataway, NJ; 1:2000). Signals were detected using the enhanced chemiluminescence system (GE Healthcare Bio-Science Corp.). Densitometric analysis was conducted using ImageJ and normalized to β -actin as loading control.

Immunofluorescence Staining on Retinal Sections

Immunostaining on retinal sections was performed as described previously [22]. Eyes were enucleated, fixed in 4% PFA (overnight at 4 °C), washed in PBS, and cryoprotected

in 30% sucrose. Cryostat sections (10 μ m) were prepared and mounted on glass slides. The sections were permeabilized in 0.05% Triton X-100 (10 min) and blocked in 10% normal goat serum for 1 h at room temperature. Sections were then incubated with primary antibodies (Table 2) overnight, followed by 1-h incubation with fluorescein-conjugated secondary antibodies (Invitrogen, Carlsbad, CA; 1:400) as previously described [22]. Sections were washed in PBS and covered with mounting medium (Vector Laboratories cat. no. H-1000, Burlingame, CA). Images were taken using a confocal microscope (LSM 780; Carl Zeiss, Thornwood, NY). Quantification of fluorescence intensities of GFAP signal was performed using ImageJ software. The analysis included measuring fluorescent signal from the nerve fiber layer of the retina to the outer limiting membrane.

Table 2 Antibodies used in the study

Antibody	Cat. no.	Company	Dilution	Experiment
Arginase 2	SC-20151	Santa Cruz, Dallas, TX	1:500	Western blotting
Bm3a	SC-31984	Santa Cruz, Dallas, TX	1:200	Immunostaining
GFAP	Z0334	Dako, Carpinteria, CA	1:200	Immunostaining
Iba1	019-19741	Wako, Richmond, VA	1:200	Immunostaining
NeuN	MAB377	Millipore, Billerica, MA	1:200	Immunostaining
p-BAD	4366	Cell Signaling, Danvers, MA	1:500	Western blotting
p-ERK1/2	4370	Cell Signaling, Danvers, MA	1:500	Western blotting
Total ERK1/2	4695	Cell Signaling, Danvers, MA	1:500	Western blotting
Synaptophysin	MABN1193	Millipore, Billerica, MA	1:200	Immunostaining
Tuj1	801202	BioLegend, San Diego, CA	1:200	Immunostaining
β -Actin	4511	Sigma-Aldrich, St. Louis, MO	1:5000	Western blotting
Calbindin	C9848	Sigma-Aldrich, St. Louis, MO	1:200	Immunostaining
ChAT	AB144P	Millipore, Billerica, MA	1:200	Immunostaining
NLRP3	15101	Cell Signaling, Danvers, MA	1:500	Western blotting
Cleaved caspase-1	SC-514	Santa Cruz, Dallas, TX	1:500	Western blotting
p-NFkB	3033	Cell Signaling, Danvers, MA	1:500	Western blotting

Retinal Flatmount Analysis

Eyeballs were collected at 60 days following EAE induction and fixed in 4% paraformaldehyde (PFA) at 4 °C overnight. Retinal flatmounts were prepared, and neuronal survival on the RGC layer was quantified as we described previously [22]. Immunostaining was performed using neuronal marker, NeuN (neuronal nuclei), and RGC specific marker, Brn3a (brain-specific homeobox/POU domain protein 3A) [26, 27]. Briefly, retinal flatmounts were incubated with antibodies (1:200 dilution) for 2 h at 37 °C and then incubated overnight with fluorescein-conjugated secondary antibodies (Invitrogen, Carlsbad, CA; 1:400). Four images per retina were taken in the mid-periphery of the ganglion cell layer (GCL) using a confocal microscope (LSM 780; Carl Zeiss, Thornwood, NY), and quantification was performed using NIH ImageJ software. Data are presented as a percentage of NeuN or Brn3a-positive cell numbers in the ganglion cell layer (GCL) relative to the WT control retinas [23]. In order to quantify microglial activation, retinal flatmounts were immunostained as described above, using Iba1 antibody, and imaged using confocal microscopy (four images per retina at the mid-periphery). Optical density was calculated using NIH ImageJ software.

Statistical Analysis

Statistical analyses were conducted using GraphPad Prism 7 (GraphPad Software Inc., La Jolla, CA). The Student's *t* test (two-tailed) was used for single comparisons, and two-way ANOVA followed by Tukey test was used for multiple comparisons. A *p* value < 0.05 was considered statistically significant. Results are presented as mean ± SEM.

Results

A2 Deletion Improved EAE-Induced Motor Deficits

EAE is a widely accepted animal model of MS. It mimics the progressive demyelination associated with MS leading to gradual paralysis in mice. In the current study, we employed an active immunization model to induce chronic EAE in WT and A2^{-/-} mice using myelin oligodendrocyte glycoprotein (MOG) peptide. EAE progression and evaluation was continued up to 60 days after induction. Animals were euthanized at different time points for analysis as depicted in Fig. 1a.

Initial signs of paralysis indicated by the loss of tail tonicity started at day 9 in WT mice. Clinical symptoms of EAE further increased gradually in WT mice, as measured by the clinical score. A slight improvement was observed between days 18 and 23, but this change was not statistically

significant. Animals displayed the most profound clinical EAE symptoms between days 28 and 33. In A2^{-/-} mice induced with EAE, appearance of the initial signs of paralysis was slightly delayed (beginning at day 11) and the clinical scores were significantly lower compared with WT EAE mice. In general, EAE-induced motor deficits were milder in A2^{-/-} EAE mice as depicted by the lower clinical scores throughout the induction period (Fig. 1b). C57B/L6 mice, unlike mice on the SJL background, are reported to develop chronic, non-relapsing EAE. While we did notice improvement of clinical scores in our WT mice, the slight recovery pattern observed in our study was not statistically significant.

Expression of A2 Is Upregulated in EAE Retinas

Changes in the expression of A2 in response to EAE induction were examined using Western blotting. A significant increase in A2 protein level was observed in the WT EAE retinas (15 days post-induction) as compared with controls (Fig. 2a, b). Immunolabeling studies showed increased A2 expression in the outer plexiform layer (OPL) and to a lesser extent in the inner nuclear layer (INL) as well as the ganglion cell layer (GCL) (Fig. 2c–f). Colocalization studies were done using markers for retinal ganglion cells (Brn3a), amacrine cells (ChAT (choline acetyl transferase)), horizontal cells (calbindin), and astrocytes (GFAP) (Fig. 2g–j). Expression of A2 was localized in calbindin, Brn3a, and ChAT-positive cells. A2 expression was not observed in GFAP-positive cells. These results are consistent with our previous studies in ischemic retinopathy models [21]. Retinas from A2^{-/-} mice did not show any expression of A2.

EAE-Induced Neurodegeneration Is Reduced in A2^{-/-} Retina

Loss of RGCs is a major feature of EAE-induced retinal injury [16, 28–30]. In the current study, EAE-induced RGC loss was investigated using retinal flatmount analysis. Representative images of flatmounts (60 days post-immunization) immunostained using the GCL marker Brn3a (Fig. 3a–d) and the neuronal marker NeuN (Fig. 3f–i) showed a marked reduction in GCL neurons in the WT EAE retinas. However, A2 deletion significantly improved the survival of the GCL neurons. Quantification of both Brn3a-positive cells (Fig. 3e) and NeuN-positive cells (Fig. 3j) in the GCL showed similar decreases of about 50% in WT EAE retinas as compared with WT controls. This EAE-induced RGC loss was significantly reduced in A2^{-/-} retinas, compared with WT, as measured by both markers. Immunostaining of retinal cryostat sections using NeuN and Brn3a demonstrated similar results (Fig. 3k–n) further confirming improved RGC survival in A2^{-/-} EAE retinas.

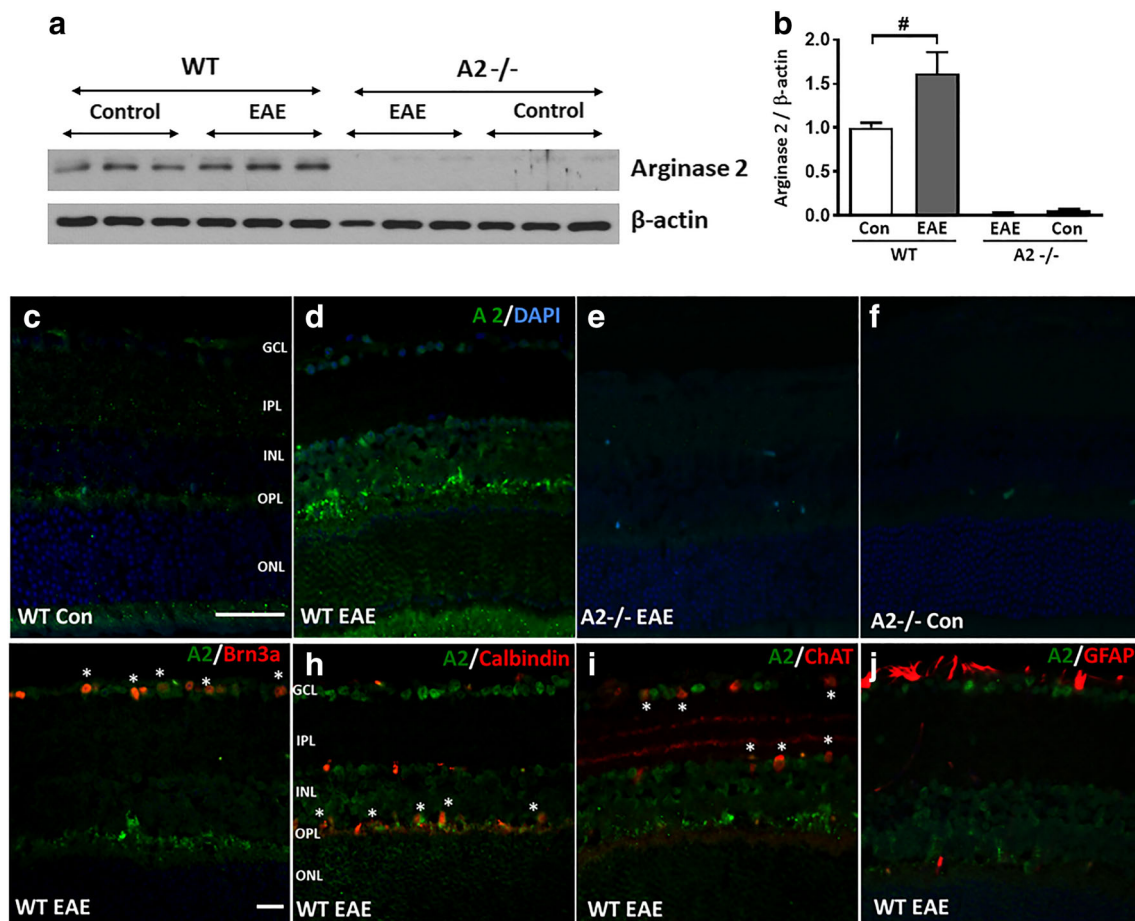


Fig. 2 Expression of arginase 2 is increased in the WT EAE retina. **a, b** Western blotting and quantification showed a significant increase in A2 expression in the WT EAE retinas at 14-day post-immunization as compared with WT control. **c–f** Representative immunofluorescence images showing increased expression of A2 in WT EAE retina as

compared with WT control. No expression of A2 is observed in A2^{-/-} retinas. **g–j** Colocalization studies showing expression of A2 in retinal ganglion cells (Brn3a), amacrine cells (ChAT), and horizontal cells (calbindin). Asterisks indicate areas of colocalization. Scale bar 50 μm. Data are presented as mean ± SEM. [#]*p* < 0.05. *N* = 4–5

Immunofluorescence studies on retinal sections (60 days post-induction) using Tuj1 (Fig. 4a–d) and synaptophysin (Fig. 4e–h) antibodies further support EAE-induced degeneration of retinal neurons. A marked reduction in the Tuj1 immunostaining observed in WT EAE retinas indicated the axonal loss in response to EAE treatment. A2 deletion improved the levels of Tuj1 expression in the EAE retinas in comparison with WT EAE retinas. Synaptophysin (a pre-synaptic marker) immunostaining was performed to examine loss of synapses due to neuronal injury in the EAE model [31]. Marked thinning of the synaptic zone (evidenced by around 36% decrease in the thickness of synaptophysin signal) in the inner plexiform layer (IPL) of WT EAE retinas indicated a reduction of synaptic contacts in the WT EAE retina. Deletion of A2 improved the IPL synaptic zone thickness in the EAE retina (around 27% compared with control retinas), suggesting improved synaptic contacts.

Analysis of EAE-Induced Retinal Thinning

EAE-induced changes in retinal structure were examined in live mice (50 days post-induction) using OCT (Fig. 5a–d). Similar to previous reports [17], EAE mice exhibited significant retinal thinning as compared with the control group. The thinning was pronounced in total retina and the ganglion cell complex (GCC: RNFL + GCL + IPL) thickness. A2^{-/-} EAE retinas showed a trend towards the preservation of retinal thickness; however, this did not reach statistical significance (Fig. 5e, f).

A2 Deletion Ameliorates EAE-Induced Glial Alterations After EAE

Activation of glial cells has been previously reported in EAE mice [32]. In the current study, we examined GFAP immunostaining as a marker of macroglial activation in retinal cryostat

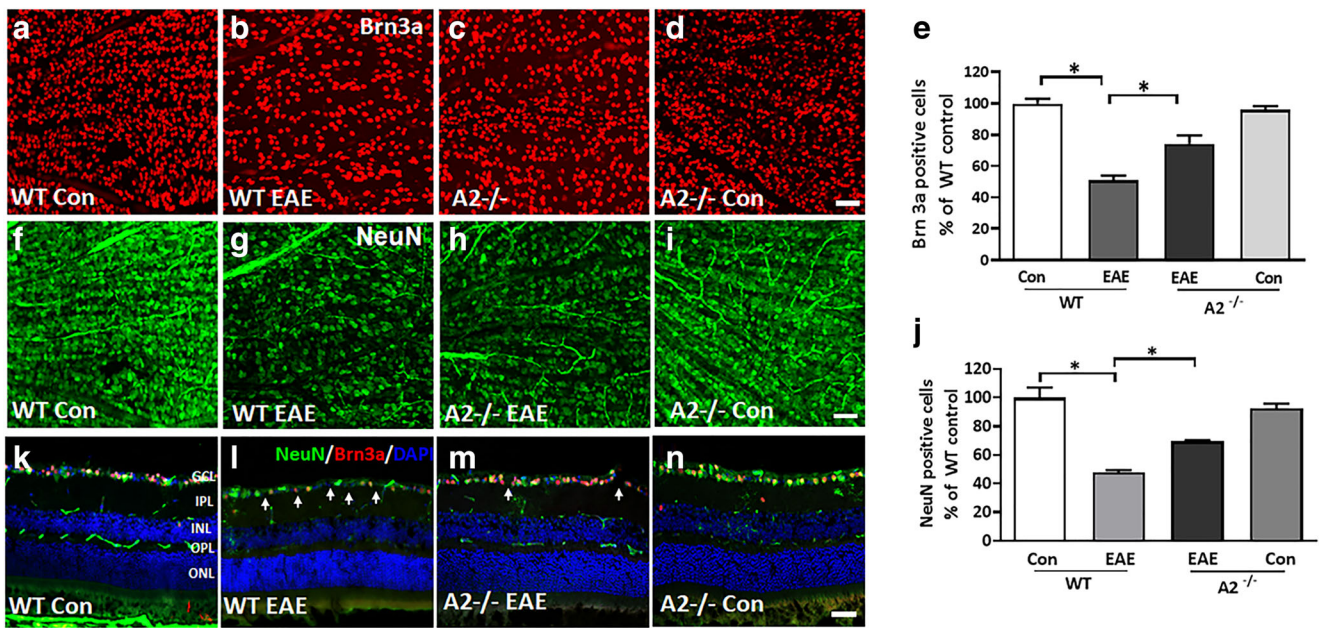


Fig. 3 A2 deletion protects against EAE-induced RGC loss. Representative confocal images showing the immunolabeling of retinal flat mounts with Brn3a (a–d) and NeuN in the GCL layer (f–i). Quantitative analysis demonstrating significant loss of NeuN-positive (e) and Brn3a-positive (j) cells in the GCL in response to EAE induction. A2 deletion significantly protected against the EAE-induced neuronal loss. Data are presented as mean ± SEM. **p* < 0.01.

N = 6–7 per group. Scale bar 50 μm. k–n Confocal images of retinal cryostat sections immunostained with NeuN, Brn3a, and DAPI. Arrows indicate areas of cell loss. Scale bar 50 μm. GCL ganglion cell layer, INL inner nuclear layer, IPL inner plexiform layer, ONL outer nuclear layer, OPL outer plexiform layer. *N* = 4–6, and representative images are presented

sections from WT and A2^{-/-} EAE mice and their respective controls (Fig. 6a–d). WT EAE retinas showed increased

GFAP expression beyond the Müller cell end-feet into the inner retina layers. A2^{-/-} EAE retinas showed decreased

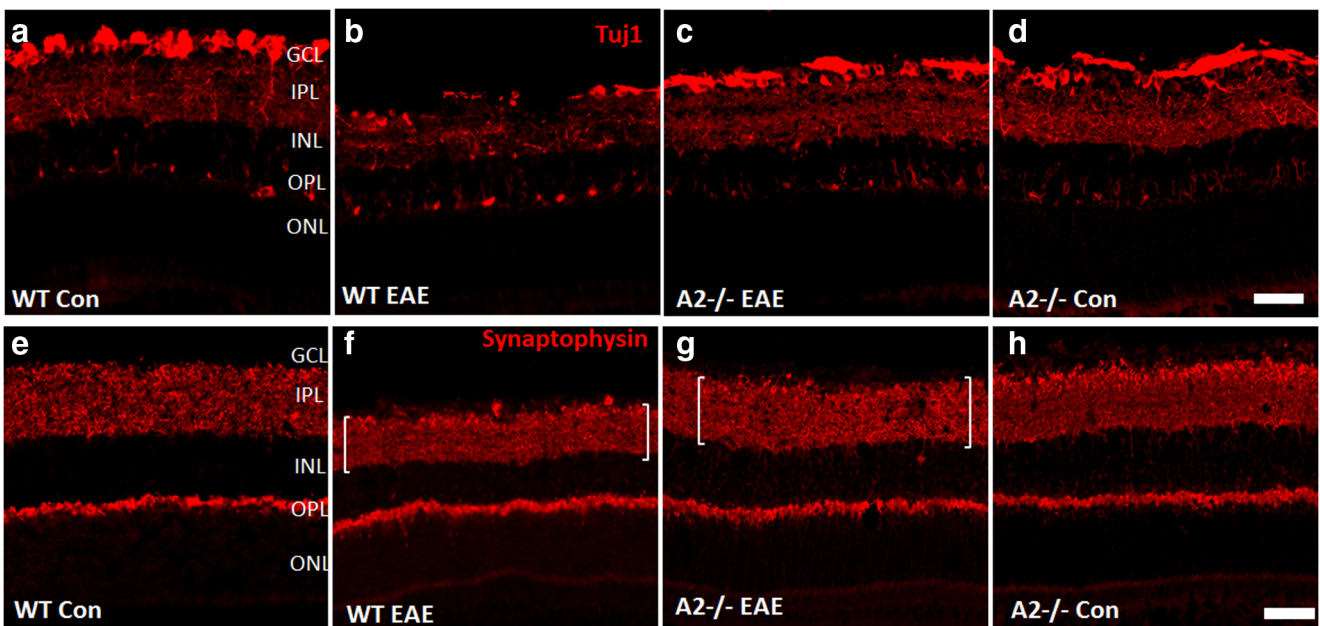


Fig. 4 EAE-induced neurodegeneration in the inner retina is decreased by A2 deletion. Confocal images of retinal cryostat sections showing the immunolabeling of Tuj1 (a–d), a marker for RGCs and their axons, and synaptophysin (e–h), a pre-synaptic marker. A marked reduction is observed in the expression of both Tuj1 and synaptophysin in WT EAE retina, while A2 deletion markedly improved their levels. EAE-induced

downregulation of both markers was markedly improved in A2 retinas. Brackets indicate synaptic zone thickness. Scale bar 100 μm. GCL ganglion cell layer, INL inner nuclear layer, IPL inner plexiform layer, ONL outer nuclear layer, OPL outer plexiform layer. *N* = 4–6, and representative images are presented

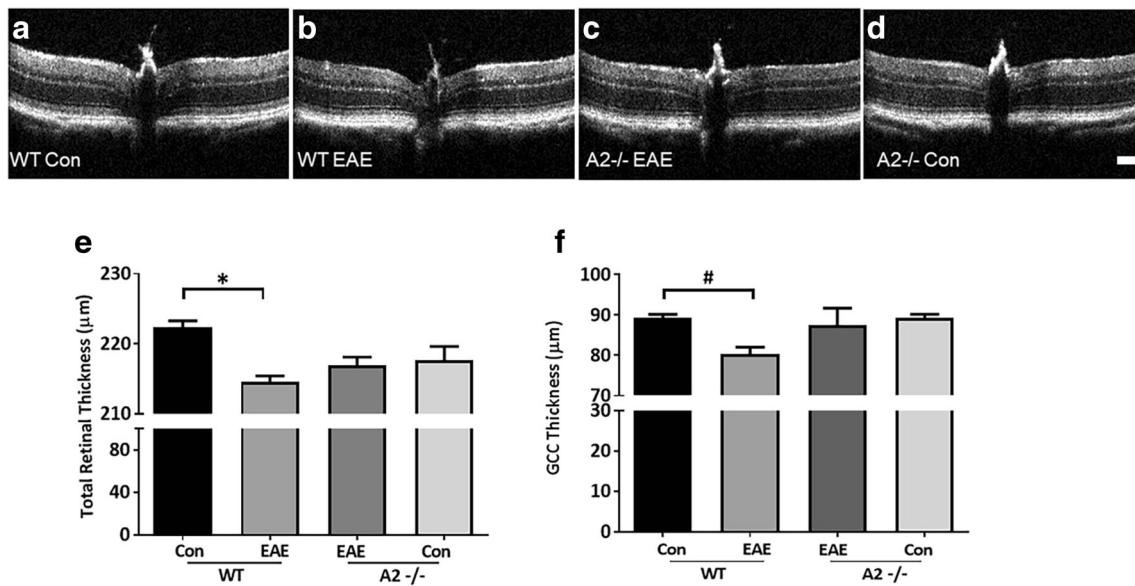


Fig. 5 EAE-induced retinal thinning is abrogated by A2 deletion. **a–d** Representative B-scan images from control and EAE retinas, using spectral domain-optical coherence tomography (SD-OCT). Scale bar 100 μm. **e–f** Quantitative analysis showing significant reduction in the thickness of total retina and GCC (ganglion cell complex) in

WT EAE compared with WT controls. These changes are partially rescued in the retinas of the A2^{-/-} mice, but the differences are not statistically significant. Data are presented as mean ± SEM. * $p < 0.01$; # $p < 0.05$. $N = 8–13$

GFAP expression as compared with WT EAE which was confirmed by the quantification of the GFAP fluorescence signal using ImageJ software (Fig. 6e).

Deletion of A2 Reduced EAE-Induced Inflammatory Response

We next investigated the changes in EAE-induced retinal inflammatory response in relation to A2 deletion (Fig. 7). Analysis of mRNA levels using qPCR showed downregulation of proinflammatory genes interleukin (IL-) 12 α , C-C motif chemokine ligand 2 (CCL2), and cyclooxygenase 2 (COX2) in A2^{-/-} EAE retinas as compared with WT EAE retinas. A2 deletion increased the anti-inflammatory molecule IL-10 and arginase 1 (A1) levels in EAE retinas but did not affect the expression of IL-18 or tumor necrosis factor (TNF) α as compared with WT EAE retinas. Further, we investigated microglial activation as a measure of the inflammatory response in retinal sections at 30 days (Fig. 8a–d) and 60 days (Fig. 8e–h) following EAE induction. Consistent with the increased inflammatory response, WT EAE retinas showed increased microglial activation at both time points studied, as visualized by Iba1 immunostaining. A2 deletion ameliorated the EAE-induced microglial activation. Quantification of Iba1 immunofluorescence on retinal flatmounts demonstrated decreases in Iba1 levels in A2^{-/-} EAE retinas as compared with WT EAE retinas (Fig. 8i–k). Studies on inflammasome signaling showed significantly increased expression of cleaved caspase-1 in WT EAE; however, A2 deletion did not alter this upregulation. Changes observed in p-NF κ B and NLRP3 were

not statistically significant in either WT EAE or A2^{-/-} retinas compared with the controls (Fig. S1).

EAE-Induced Stress Signaling Is Reduced in the A2 Retina

Studies of EAE-induced stress activation were performed using Western blotting on retinal samples collected 15 days post-induction. Western blotting analysis revealed an increase in the stress marker p-ERK 1/2 (Fig. 9a–c) in the WT EAE retinas compared with WT controls. Conversely, BAD phosphorylation was significantly decreased in the WT EAE retinas (Fig. 9a, d), suggesting a reduction in prosurvival signals. These changes were reversed with A2 deletion reflecting a decrease in stress and an increase in survival signaling in A2^{-/-} retinas following EAE induction. Differences in the prosurvival marker p-Akt were not observed (data not shown).

Discussion

Using a well-established experimental model of MS, the current study was undertaken to investigate the impact of A2 deletion in the EAE retina. Our results demonstrate the protective effect of A2 deficiency against EAE-induced neurodegeneration. In response to EAE, mice lacking A2 showed increased RGC survival, improved synaptic contacts, reduced retinal inflammatory response, decreased glial activation, together with improved motor skills, compared with their WT counterparts. To the best of our knowledge, this is the first

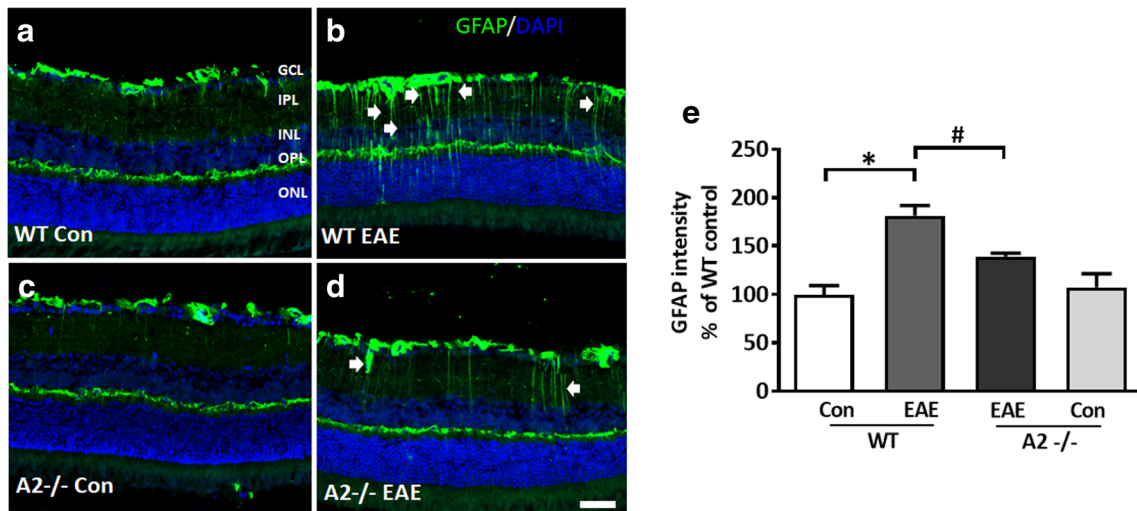


Fig. 6 A2 deletion ameliorates EAE-induced glial activation. **a–d** Immunofluorescence staining of retinal sections (60 days post-immunization) using GFAP antibody, demonstrating activation of glial cells in the WT EAE retina. Deletion of A2 markedly reduced this effect. Arrows indicate activated Muller cell processes. **e** Quantification of the GFAP immunofluorescence intensity (from nerve fiber layer to outer

limiting membrane) showing the increased GFAP level in the WT EAE retinal sections. A2 deletion significantly reduced this effect. $N=4-6$, and representative images are presented. GCL ganglion cell layer, IPL inner plexiform layer, INL inner nuclear layer, OPL outer plexiform layer, ONL outer nuclear layer. Scale bar 50 μm . Data are presented as mean \pm SEM. * $p < 0.01$; # $p < 0.05$

report demonstrating the impact of A2 deletion on the EAE-induced neurodegeneration in the retina.

The C57BL/6 mouse model of MOG-induced chronic EAE has been extensively used by several laboratories to study optic neuritis and neurodegeneration in the retina [16, 19, 30, 33]. Similar to other studies, EAE-induced motor deficits were clearly evident in WT mice [16, 19, 32]. Moreover, our results

demonstrated that A2 deletion significantly improved the clinical symptoms. Our data support a recent study by Choudry et al. [34] in which EAE-induced inflammatory changes were studied in spinal cord tissues. The authors showed improved clinical score in A2^{-/-} EAE mice similar to our findings, and they additionally reported a marked delay in the onset of clinical score symptoms in the A2^{-/-} mice. The discrepancy in the

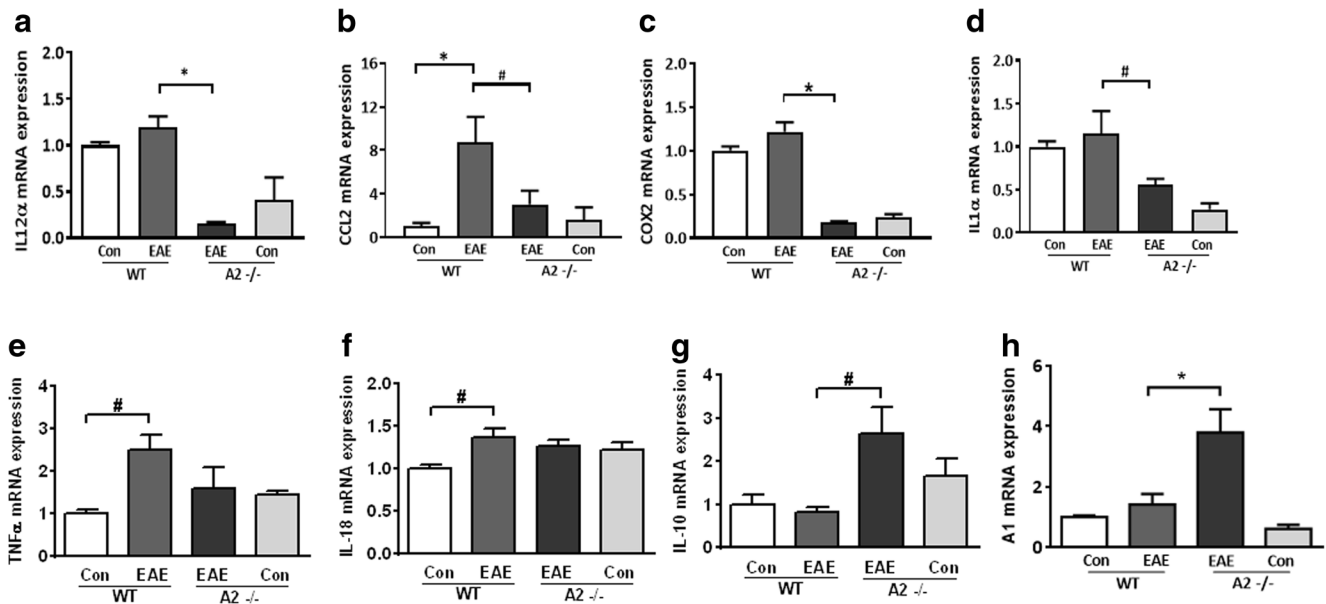


Fig. 7 A2 deletion suppresses EAE-induced inflammatory response. **a–d** RT-PCR analysis demonstrating changes in mRNA levels of proinflammatory cytokines and chemokines in EAE retinas (30 days post-immunization). IL-12 α (**a**), CCL2 (**b**), COX2 (**c**), and IL-1 α (**d**) mRNA levels were markedly reduced by A2 deletion in EAE groups.

e–f EAE-induced increases in TNF α and IL-18 were not affected by A2 deletion. **g–h** A2 deletion significantly increased the anti-inflammatory molecules IL-10 and A1 as compared with WT EAE and control groups. Data are presented as mean \pm SEM. * $p < 0.01$; # $p < 0.05$. $N=3-10$

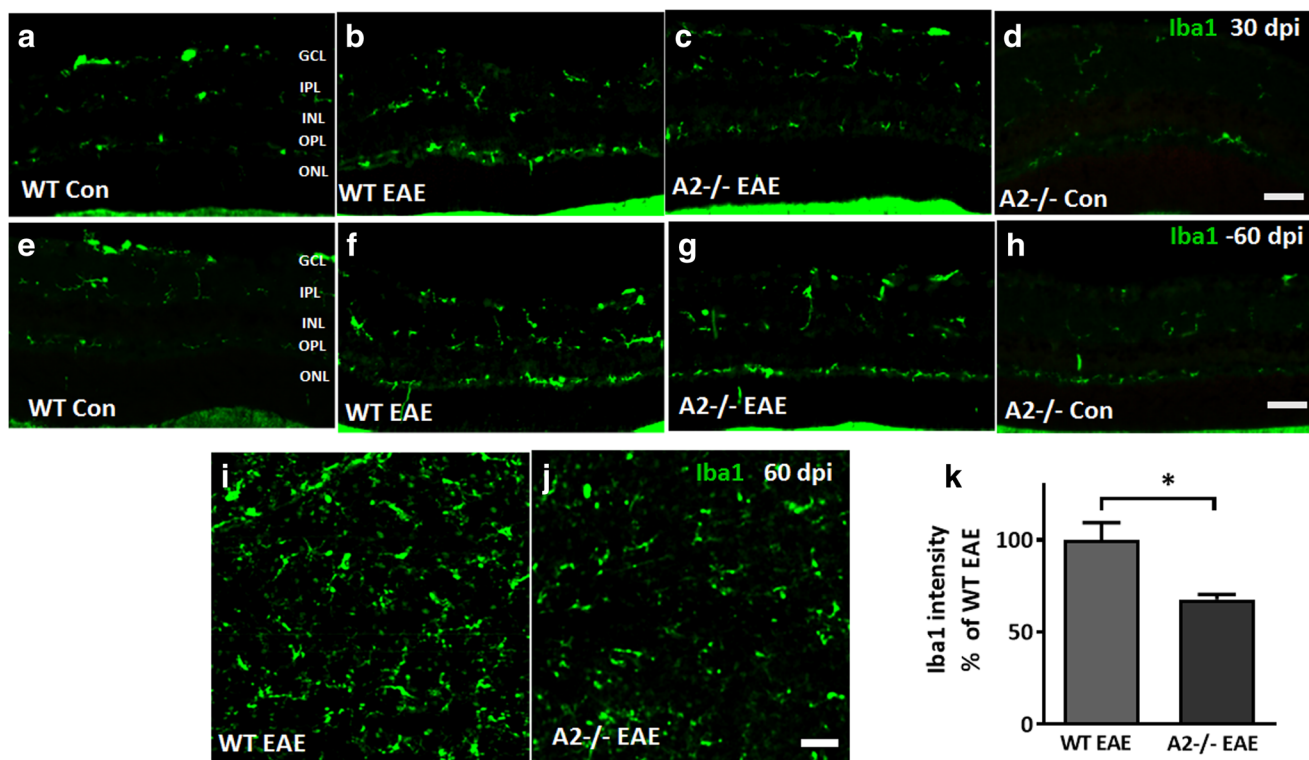


Fig. 8 A2 deletion ameliorates EAE-induced microglial activation. **a–d** Immunofluorescence staining for Iba1 (a microglia/macrophage marker) on retinal sections (30 days post-immunization (dpi)) showed increased microglial activation in the WT EAE retina. A2^{-/-} EAE retina showed reduced microglial activation. EAE-induced microglial activation continued to be observed in WT EAE retina at 60 days post-immunization (dpi); A2 deletion reduced this activation (**e–h**). $N=4–6$,

and representative images are presented. GCL ganglion cell layer, IPL inner plexiform layer, INL inner nuclear layer, OPL outer plexiform layer, ONL outer nuclear layer. Scale bar 50 μ m. **i–j** Iba1 immunostaining on retinal flatmounts from WT EAE and A2^{-/-} EAE retinas. **k** Quantification of Iba1 fluorescence intensity on retinal flat mounts showing significant downregulation in the A2^{-/-} EAE group as compared with WT EAE. Data are presented as mean \pm SEM. * $p < 0.01$. Scale bar 50 μ m

onset between the two studies could be due to the difference in the timing of PTX administration (days 0 and 2 versus days 0 and 1 in our study), the age of mice at induction (9 weeks versus 12 weeks in our study), and housing conditions [34].

The upregulation of A2 observed in the EAE retina is consistent with our findings in other retinal neurodegenerative models suggesting that A2 plays an important role in retinal disease pathology [21–23]. More specifically, the localization data showing expression of A2 in the OPL in the EAE retinas is similar to what we have previously reported in the OIR mouse model [21]. Degeneration of RGCs is a characteristic feature of the EAE retina and is a major cause of visual dysfunction in MS patients [16]. Similar to the findings from other laboratories [16, 32, 35, 36], we have observed a significant reduction in RGCs in the EAE retina. This RGC loss was significantly abrogated by A2 deletion. The retinal neuroprotection with A2 deletion observed in the EAE mice is comparable with our previous results in other models of retinal neurodegeneration such as OIR, IR, and ONC [21–23]. Quantification of RGC loss with the neuronal marker, NeuN, and the specific RGC marker, Brn3a, showed comparable results. This suggests that the neurodegeneration is mostly due to RGC loss, which is in agreement with previously

published literature on EAE model [16, 32, 35, 36]. Moreover, A2^{-/-} retinas exhibited preserved RGC axons and neuronal synapses as measured by Tuj1 and synaptophysin immunostaining on retinal sections. Interestingly, the neuroprotection in A2^{-/-} retinas did not translate significantly in the preservation of inner retinal thickness (studied by SD-OCT) as compared with WT EAE retinas. The current study did not evaluate visual function in the EAE mice, and hence, it is not yet clear whether preservation of RGCs in the A2^{-/-} retina improved visual function. We are planning to address this issue in our future studies.

We have previously reported that A2 deletion leads to a reduction in retinal inflammatory responses [21–23, 37]. In the present study, A2 deletion was associated with decreased mRNA levels for inflammatory genes (IL-1 α , IL-12 α , CCL2, and COX2) that have been reported to be involved in EAE pathology [38–41]. Interestingly, marked reductions in the level of COX2 and IL-1 α were observed in the A2^{-/-} control retinas compared with WT controls. Induction of EAE did not significantly alter the levels of these mRNAs in A2^{-/-} retinas. This decreased inflammatory response in A2^{-/-} retinas was associated with reduced microglial activation manifested by reduced Iba1 immunofluorescence. Inflammasome activation

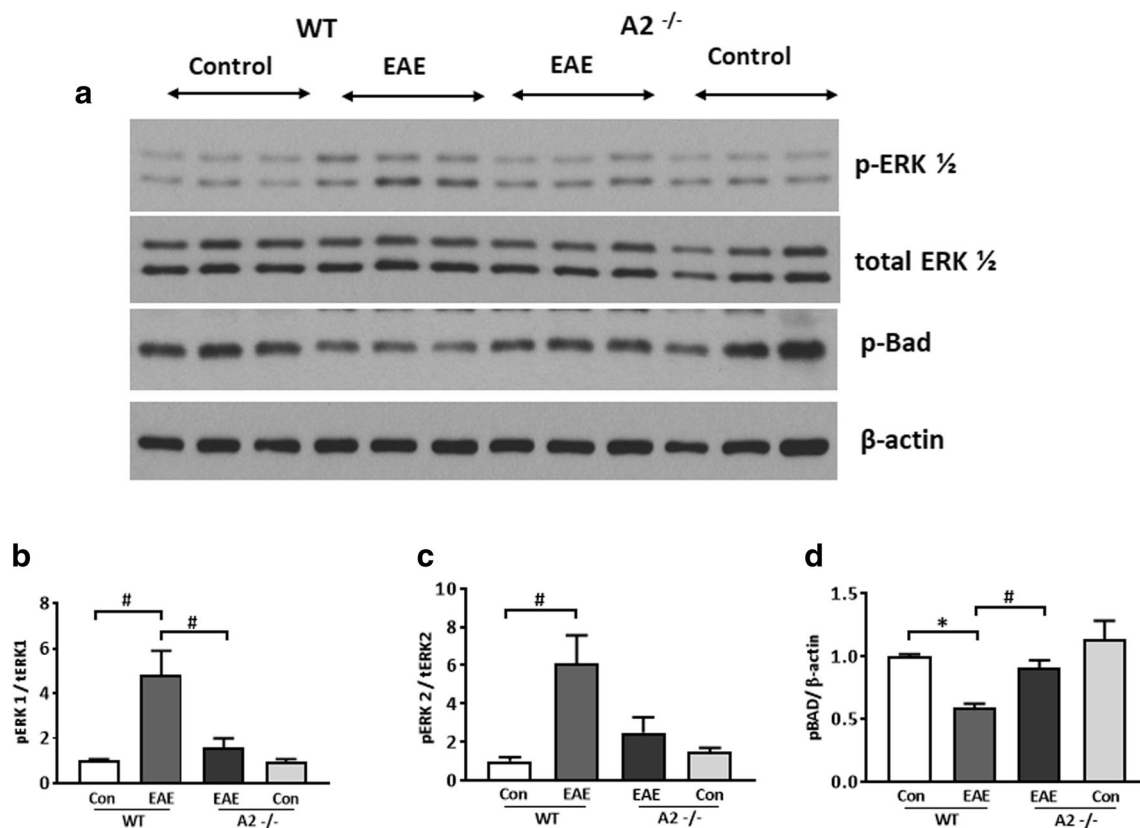


Fig. 9 Deletion of A2 reduced EAE-induced stress signaling in the retina. **a** Western blot studies showing increased levels of p-ERK1/2 and reduced p-BAD levels in WT EAE retina. These changes were reversed in A2^{-/-} EAE retina. **b–d** Quantitative analysis of Western blots demonstrate significantly increased levels of p-ERK1/2 and reduced levels of p-

BAD in the WT EAE retina compared with WT control. Deletion of A2 altered the EAE-induced increase in p-ERK1 levels and reduction in p-BAD levels. Data are presented as mean \pm SEM. * $p < 0.01$; # $p < 0.05$. $N = 3–6$

is reported in EAE [42, 43]. However, A2 deletion did not alter the levels of IL-18, TNF α , p-NFkB, NLRP3, or cleaved caspase-1, compared with WT EAE. These results suggest that neuroprotective effects conferred by A2 deletion could be independent of inflammasome signaling in the EAE retina. Further studies are needed to confirm this observation. The current study did not evaluate T cell infiltration in the EAE retina. Our future study will investigate whether A2 deletion impacts T cell infiltration or alters T cell interaction with microglia. Activation of Müller glia is considered as an indication of retinal injury during a disease or stress condition and is manifested in retinal neurodegenerative conditions [44]. Our results are consistent with previous reports showing activation of macroglia in response to EAE induction [32]. The reduced GFAP levels observed in A2^{-/-} retina is consistent with decreased retinal inflammation and injury in response to EAE.

In the current study, A2^{-/-} mice subjected to EAE showed a reduction in phosphorylation of ERK and an increase in phosphorylation of BAD. Activation of ERK signaling in the EAE model has been reported by others to be associated with the inflammatory response [45–47]. In our study, reduction in ERK activation in A2^{-/-} retina suggests a role for A2 in EAE-induced retinal inflammation, in addition to its cytotoxic

effects. Consistent with our results, decreases in p-BAD have been reported [48], suggesting a decrease in prosurvival signaling during EAE. BAD is proapoptotic member of the Bcl-2 family that promotes cell death by displacing Bax from binding to Bcl-2 and Bcl-xL. Phosphorylation of BAD at serine 112 or 136 promotes cell survival by binding to 14-3-3 proteins and thus preventing the association of BAD with Bcl-2 and Bcl-xL [49]. Akt phosphorylates BAD at serine 136, and the serine 112 phosphorylation is by p90RSK [50, 51]. Changes in other survival molecules such as p-Akt have been reported in EAE [52, 53]. However, we did not observe any changes in p-Akt in the present study (data not shown). This could be due to differences in analysis time points and/or differences in the experimental model employed.

Similar to our findings, another study using the non-specific arginase inhibitor, amino-6-boronohexanoic acid (ABH), showed a milder EAE disease course and reduced inflammatory response with arginase inhibition [54]. The study by Choudry et al. [34] using the global A2^{-/-} mice suggested that A2 in dendritic cells may be promoting EAE via increased production of Th17-differentiating cytokines. Interestingly, they did not detect changes in A1 with A2 deletion. In our hands, we found significant upregulation of A1

mRNA in A2^{-/-} EAE retinas which may account, at least partly, for the protective effects seen with A2 deletion. Our future studies will be directed to address the possible interaction between the two isoforms of arginase after EAE in retinal tissue and their relation to the nitric oxide synthase (NOS) enzymes, which share the same substrate, L-arginine.

Lack of evidence for specific signaling pathways regulated by A2 is a limitation of the current study. Increased oxidative stress is a key mediator in MS and optic neuritis [19, 55, 56]. There are several possible sources of reactive oxygen species (ROS) or reactive nitrogen species (RNS) in MS and EAE such as activation of microglia and macrophages and altered function of nitric oxide synthase (NOS) to produce superoxide. Studies have shown that expression of inducible NOS (iNOS) as well as activation of microglia is enhanced in MS lesions and EAE animals [57–59]. As such, the role of iNOS has been studied in EAE with conflicting reports on a protective versus a pathologic role of the iNOS enzyme and its product, nitric oxide (NO) [60–62]. Studies performed on cerebrospinal fluid and plasma samples have demonstrated iNOS and arginase as key players of neuroinflammation in EAE rats [63]. Our investigations in diabetic retinopathy model showed increases in superoxide and peroxynitrite formation subsequent to increased arginase activity [64, 65]. Our studies in the OIR model have identified altered polyamine metabolism (by spermine oxidase) downstream of the arginase signaling pathway, as a source of oxidative stress and damage to retinal neurons [37]. In the future studies, we will be investigating the specific signaling mechanisms regulated by A2 in mediating neuroinflammation in the EAE retina.

In conclusion, our data show that A2 is critically involved in EAE-induced retinal neurodegeneration and inflammatory response. Targeting arginase signaling could be a potential therapeutic strategy for treatment of optic neuritis in MS patients.

Author Contributions CDP implemented the experiments, analyzed the data, prepared the figures, and edited the manuscript. AYF helped with experimental design, analyzed the data, prepared figures, and wrote the manuscript. FL performed experiments, analyzed the data, and prepared the figures. ZX induced the in vivo experimental model and helped with analyzing the data. EM helped with induction of the model and clinical scoring. SG helped with experimental design and establishing the animal model in our laboratory. SBS provided assistance with SD-OCT experiment and edited the manuscript. RBC contributed to experimental design and revised the manuscript. SPN conceived, designed and coordinated the experiments, and finalized the manuscript.

Funding This study was supported in part by the National Multiple Sclerosis Society (PP-1606-08778 to S.P.N.), National Eye Institute (R01EY028569 to S.P.N.), and Augusta University Culver Vision Discovery Institute.

Compliance with Ethical Standards

Conflict of Interest The authors declare that they have no conflict of interest.

References

- Balcer LJ, Miller DH, Reingold SC, Cohen JA (2015) Vision and vision-related outcome measures in multiple sclerosis. *Brain* 138: 11–27
- Sakai RE, Feller DJ, Galetta KM, Galetta SL, Balcer LJ (2011) Vision in multiple sclerosis: the story, structure-function correlations, and models for neuroprotection. *J Neuroophthalmol* 31: 362–373
- Galetta SL, Villoslada P, Levin N, Shindler K, Ishikawa H, Parr E, Cadavid D, Balcer LJ (2015) Acute optic neuritis: unmet clinical needs and model for new therapies. *Neurol Neuroimmunol Neuroinflamm* 2:e135
- Sakai T, Ishihara T, Higaki M, Akiyama G, Tsuneoka H (2011) Therapeutic effect of stealth-type polymeric nanoparticles with encapsulated betamethasone phosphate on experimental autoimmune uveoretinitis. *Invest Ophthalmol Vis Sci* 52:1516–1521
- Walter SD, Ishikawa H, Galetta KM, Sakai RE, Feller DJ, Henderson SB, Wilson JA, Maguire MG et al (2012) Ganglion cell loss in relation to visual disability in multiple sclerosis. *Ophthalmology* 119:1250–1257
- Abel LA, Bowman EA, Velakoulis D, Fahey MC, Desmond P, Macfarlane MD, Looi JCL, Adamson CL et al (2012) Saccadic eye movement characteristics in adult niemann-pick type c disease: relationships with disease severity and brain structural measures. *PLoS One* 7:e50947
- Paty DW, Li DK (1993) Interferon beta-1b is effective in relapsing-remitting multiple sclerosis. II. Mri analysis results of a multicenter, randomized, double-blind, placebo-controlled trial. Ubc ms/mri study group and the ifnb multiple sclerosis study group. *Neurology* 43:662–667
- Polman CH, O'Connor PW, Havrdova E, Hutchinson M, Kappos L, Miller DH, Phillips JT, Lublin FD et al (2006) A randomized, placebo-controlled trial of natalizumab for relapsing multiple sclerosis. *N Engl J Med* 354:899–910
- Thomas K, Proschmann U, Ziemssen T (2017) Fingolimod hydrochloride for the treatment of relapsing remitting multiple sclerosis. *Expert Opin Pharmacother* 18:1649–1660
- Thomas RH, Wakefield RA (2015) Oral disease-modifying therapies for relapsing-remitting multiple sclerosis. *Am J Health Syst Pharm* 72:25–38
- Robinson AP, Harp CT, Noronha A, Miller SD (2014) The experimental autoimmune encephalomyelitis (eae) model of ms: utility for understanding disease pathophysiology and treatment. *Handb Clin Neurol* 122:173–189
- Constantinescu CS, Farooqi N, O'Brien K, Gran B (2011) Experimental autoimmune encephalomyelitis (eae) as a model for multiple sclerosis (ms). *Br J Pharmacol* 164:1079–1106
- Nath N, Khan M, Paintlia MK, Singh I, Hoda MN, Giri S (2009) Metformin attenuated the autoimmune disease of the central nervous system in animal models of multiple sclerosis. *J Immunol* 182: 8005–8014
- Talla V, Yu H, Chou TH, Porciatti V, Chiodo V, Boye SL, Hauswirth WW, Lewin AS et al (2013) Ndh-dehydrogenase type-2 suppresses irreversible visual loss and neurodegeneration in the eae animal model of ms. *Mol Ther* 21:1876–1888
- Brambilla R, Dvorianchikova G, Barakat D, Ivanov D, Bethea JR, Shestopalov VI (2012) Transgenic inhibition of astroglial nf-kappab protects from optic nerve damage and retinal ganglion cell loss in experimental optic neuritis. *J Neuroinflammation* 9:213
- Dal Monte M, Cammalleri M, Locri F, Amato R, Marsili S, Rusciano D, Bagnoli P (2018) Fatty acids dietary supplements exert anti-inflammatory action and limit ganglion cell degeneration in the retina of the eae mouse model of multiple sclerosis. *Nutrients* 10

17. Nishioka C, Liang HF, Barsamian B, Sun SW (2019) Sequential phases of rgc axonal and somatic injury in eae mice examined using dti and oct. *Mult Scler Relat Disord* 27:315–323
18. Wilmes AT, Reinehr S, Kuhn S, Pedreiturria X, Petrikowski L, Faissner S et al (2018) Laquinimod protects the optic nerve and retina in an experimental autoimmune encephalomyelitis model. *J Neuroinflammation* 15:183
19. Larabee CM, Desai S, Agasing A, Georgescu C, Wren JD, Axtell RC et al (2016) Loss of nrf2 exacerbates the visual deficits and optic neuritis elicited by experimental autoimmune encephalomyelitis. *Mol Vis* 22:1503–1513
20. Caldwell RW, Rodriguez PC, Toque HA, Narayanan SP, Caldwell RB (2018) Arginase: a multifaceted enzyme important in health and disease. *Physiol Rev* 98:641–665
21. Narayanan SP, Suwanpradid J, Saul A, Xu Z, Still A, Caldwell RW, Caldwell RB (2011) Arginase 2 deletion reduces neuro-glial injury and improves retinal function in a model of retinopathy of prematurity. *PLoS One* 6:e22460
22. Shosha E, Xu Z, Yokota H, Saul A, Rojas M, Caldwell RW, Caldwell RB, Narayanan SP (2016) Arginase 2 promotes neurovascular degeneration during ischemia/reperfusion injury. *Cell Death Dis* 7:e2483
23. Xu Z, Fouda AY, Lemtalsi T, Shosha E, Rojas M, Liu F et al (2018) Retinal neuroprotection from optic nerve trauma by deletion of arginase 2. *Front Neurosci* 12:970
24. Poisson LM, Suhail H, Singh J, Datta I, Denic A, Labuzek K, Hoda MN, Shankar A et al (2015) Untargeted plasma metabolomics identifies endogenous metabolite with drug-like properties in chronic animal model of multiple sclerosis. *J Biol Chem* 290:30697–30712
25. Fouda AY, Xu Z, Shosha E, Lemtalsi T, Chen J, Toque HA, Tritz R, Cui X et al (2018) Arginase 1 promotes retinal neurovascular protection from ischemia through suppression of macrophage inflammatory responses. *Cell Death Dis* 9:1001
26. Rodriguez AR, de Sevilla Muller LP, Brecha NC (2014) The rna binding protein rbpms is a selective marker of ganglion cells in the mammalian retina. *J Comp Neurol* 522:1411–1443
27. Nadal-Nicolas FM, Jimenez-Lopez M, Sobrado-Calvo P, Nieto-Lopez L, Canovas-Martinez I, Salinas-Navarro M et al (2009) Bm3a as a marker of retinal ganglion cells: qualitative and quantitative time course studies in naive and optic nerve-injured retinas. *Invest Ophthalmol Vis Sci* 50:3860–3868
28. Liu Q, Li H, Yang J, Niu X, Zhao C, Zhao L, Wang Z (2017) Valproic acid attenuates inflammation of optic nerve and apoptosis of retinal ganglion cells in a rat model of optic neuritis. *Biomed Pharmacother* 96:1363–1370
29. Smith AW, Rohrer B, Wheless L, Samantaray S, Ray SK, Inoue J, Azuma M, Banik NL (2016) Calpain inhibition reduces structural and functional impairment of retinal ganglion cells in experimental optic neuritis. *J Neurochem* 139:270–284
30. Azuchi Y, Kimura A, Guo X, Akiyama G, Noro T, Harada C, Nishigaki A, Namekata K et al (2017) Valproic acid and ask1 deficiency ameliorate optic neuritis and neurodegeneration in an animal model of multiple sclerosis. *Neurosci Lett* 639:82–87
31. Gudi V, Gai L, Herder V, Tejedor LS, Kipp M, Amor S, Sühs KW, Hansmann F et al (2017) Synaptophysin is a reliable marker for axonal damage. *J Neuropathol Exp Neurol* 76:109–125
32. Horstmann L, Schmid H, Heinen AP, Kurschus FC, Dick HB, Joachim SC (2013) Inflammatory demyelination induces glia alterations and ganglion cell loss in the retina of an experimental autoimmune encephalomyelitis model. *J Neuroinflammation* 10:120
33. Niwa M, Aoki H, Hirata A, Tomita H, Green PG, Hara A (2016) Retinal cell degeneration in animal models. *Int J Mol Sci* 17
34. Choudry M, Tang X, Santorian T, Wasnik S, Xiao J, Xing W, Lau KHW, Mohan S et al (2018) Deficient arginase ii expression without alteration in arginase i expression attenuated experimental autoimmune encephalomyelitis in mice. *Immunology*. 155:85–98
35. Guan Y, Shindler KS, Tabuena P, Rostami AM (2006) Retinal ganglion cell damage induced by spontaneous autoimmune optic neuritis in mog-specific tcr transgenic mice. *J Neuroimmunol* 178:40–48
36. Quinn TA, Dutt M, Shindler KS (2011) Optic neuritis and retinal ganglion cell loss in a chronic murine model of multiple sclerosis. *Front Neurol* 2:50
37. Narayanan SP, Xu Z, Putluri N, Sreekumar A, Lemtalsi T, Caldwell RW, Caldwell RB (2014) Arginase 2 deficiency reduces hyperoxia-mediated retinal neurodegeneration through the regulation of polyamine metabolism. *Cell Death Dis* 5:e1075
38. Muthian G, Raikwar HP, Johnson C, Rajasingh J, Kalgutkar A, Marnett LJ, Bright JJ (2006) Cox-2 inhibitors modulate il-12 signaling through jak-stat pathway leading to th1 response in experimental allergic encephalomyelitis. *J Clin Immunol* 26:73–85
39. dos Santos AC, Barsante MM, Arantes RM, Bernard CC, Teixeira MM, Carvalho-Tavares J (2005) Ccl2 and ccl5 mediate leukocyte adhesion in experimental autoimmune encephalomyelitis—an intravital microscopy study. *J Neuroimmunol* 162:122–129
40. Sutton C, Brereton C, Keogh B, Mills KH, Lavelle EC (2006) A crucial role for interleukin (il)-1 in the induction of il-17-producing t cells that mediate autoimmune encephalomyelitis. *J Exp Med* 203:1685–1691
41. Grifka-Walk HM, Giles DA, Segal BM (2015) Il-12-polarized th1 cells produce gm-csf and induce eae independent of il-23. *Eur J Immunol* 45:2780–2786
42. Barclay W, Shinohara ML (2017) Inflammasome activation in multiple sclerosis and experimental autoimmune encephalomyelitis (eae). *Brain Pathol* 27:213–219
43. McKenzie BA, Mamik MK, Saito LB, Boghazian R, Monaco MC, Major EO et al (2018) Caspase-1 inhibition prevents glial inflammasome activation and pyroptosis in models of multiple sclerosis. *Proc Natl Acad Sci U S A* 115:E6065–E6074
44. de Hoz R, Rojas B, Ramirez AI, Salazar JJ, Gallego BI, Trivino A et al (2016) Retinal macroglial responses in health and disease. *Biomed Res Int* 2016:2954721
45. Bao J, Zhu J, Luo S, Cheng Y, Zhou S (2016) Cxcr7 suppression modulates microglial chemotaxis to ameliorate experimentally-induced autoimmune encephalomyelitis. *Biochem Biophys Res Commun* 469:1–7
46. Lu L, Zhang X, Tong H, Zhang W, Xu P, Qu S (2017) Central administration of 5z-7-oxozeaenol protects experimental autoimmune encephalomyelitis mice by inhibiting microglia activation. *Front Pharmacol* 8:789
47. Birkner K, Wasser B, Loos J, Plotnikov A, Seger R, Zipp F, Witsch E, Bittner S (2017) The role of erk signaling in experimental autoimmune encephalomyelitis. *Int J Mol Sci* 18
48. Das A, Guyton MK, Butler JT, Ray SK, Banik NL (2008) Activation of calpain and caspase pathways in demyelination and neurodegeneration in animal model of multiple sclerosis. *CNS Neurol Disord Targets* 7:313–320
49. Zha J, Harada H, Yang E, Jockel J, Korsmeyer SJ (1996) Serine phosphorylation of death agonist bad in response to survival factor results in binding to 14-3-3 not bcl-x(l). *Cell*. 87:619–628
50. del Peso L, Gonzalez-Garcia M, Page C, Herrera R, Nunez G (1997) Interleukin-3-induced phosphorylation of bad through the protein kinase akt. *Science*. 278:687–689
51. Bonni A, Brunet A, West AE, Datta SR, Takasu MA, Greenberg ME (1999) Cell survival promoted by the ras-mapk signaling pathway by transcription-dependent and -independent mechanisms. *Science*. 286:1358–1362
52. Hobom M, Storch MK, Weissert R, Maier K, Radhakrishnan A, Kramer B, Bähr M, Diem R (2004) Mechanisms and time course of neuronal degeneration in experimental autoimmune encephalomyelitis. *Brain Pathol (Zurich, Switzerland)* 14:148–157
53. Sattler MB, Merkler D, Maier K, Stadelmann C, Ehrenreich H, Bahr M et al (2004) Neuroprotective effects and intracellular

- signaling pathways of erythropoietin in a rat model of multiple sclerosis. *Cell Death Differ* 11(Suppl 2):S181–S192
54. Xu L, Hilliard B, Carmody RJ, Tsabary G, Shin H, Christianson DW, Chen YH (2003) Arginase and autoimmune inflammation in the central nervous system. *Immunology*. 110:141–148
 55. Lieven CJ, Hoegger MJ, Schlieve CR, Levin LA (2006) Retinal ganglion cell axotomy induces an increase in intracellular superoxide anion. *Invest Ophthalmol Vis Sci* 47:1477–1485
 56. Castegna A, Palmieri L, Spera I, Porcelli V, Palmieri F, Fabis-Pedrini MJ, Kean RB, Barkhouse DA et al (2011) Oxidative stress and reduced glutamine synthetase activity in the absence of inflammation in the cortex of mice with experimental allergic encephalomyelitis. *Neuroscience*. 185:97–105
 57. Giannetti P, Politis M, Su P, Turkheimer F, Malik O, Keihaninejad S, Wu K, Reynolds R et al (2014) Microglia activation in multiple sclerosis black holes predicts outcome in progressive patients: an in vivo [(11)c](r)-pk11195-pet pilot study. *Neurobiol Dis* 65:203–210
 58. Wu WF, Tan XJ, Dai YB, Krishnan V, Warner M, Gustafsson JA (2013) Targeting estrogen receptor beta in microglia and t cells to treat experimental autoimmune encephalomyelitis. *Proc Natl Acad Sci U S A* 110:3543–3548
 59. Howell OW, Rundle JL, Garg A, Komada M, Brophy PJ, Reynolds R (2010) Activated microglia mediate axoglial disruption that contributes to axonal injury in multiple sclerosis. *J Neuropathol Exp Neurol* 69:1017–1033
 60. Dalton DK, Wittmer S (2005) Nitric-oxide-dependent and independent mechanisms of protection from CNS inflammation during th1-mediated autoimmunity: evidence from eae in inos ko mice. *J Neuroimmunol* 160:110–121
 61. Farias AS, de la Hoz C, Castro FR, Oliveira EC, Ribeiro dos Reis JR, Silva JS et al (2007) Nitric oxide and tnfa effects in experimental autoimmune encephalomyelitis demyelination. *Neuroimmunomodulation*. 14:32–38
 62. Staykova MA, Fordham SA, Bartell GJ, Cowden WB, Willenborg DO (2006) Nitric oxide contributes to the resistance of young sjl/j mice to experimental autoimmune encephalomyelitis. *J Neuroimmunol* 176:1–8
 63. Ljubisavljevic S, Stojanovic I, Pavlovic R, Sokolovic D, Pavlovic D, Cvetkovic T, Stevanovic I (2012) Modulation of nitric oxide synthase by arginase and methylated arginines during the acute phase of experimental multiple sclerosis. *J Neurol Sci* 318:106–111
 64. Patel C, Rojas M, Narayanan SP, Zhang W, Xu Z, Lemtalsi T et al (2013) Arginase as a mediator of diabetic retinopathy. *Front Immunol* 4:173
 65. Elms S, Chen F, Wang Y, Qian J, Askari B, Yu Y, Pandey D, Iddings J et al (2013) Insights into the arginine paradox: evidence against the importance of subcellular location of arginase and enos. *Am J Physiol Heart Circ Physiol* 305:H651–H666

Publisher's Note Springer Nature remains neutral with regard to jurisdictional claims in published maps and institutional affiliations.